| CLINICAL REPORT

Intradermal Delivery of Calcium Hydroxylapatite With Fractionated Ablation

William Driscoll[1] | Nicole M. Golbari[1] 🆔 | Alexander Vallmitjana[2] | Amanda F. Durkin[2] | Mihaela Balu[1,2] 🆔 |
Christopher B. Zachary[1]

[1]Department of Dermatology, University of California, Irvine, Irvine, California, USA | [2]Beckman Laser Institute and Medical Clinic, University of California, Irvine (UC Irvine), Irvine, California, USA

Correspondence: Mihaela Balu (mbalu@uci.edu)

ABSTRACT

Objectives: The absorption of biostimulatory particulate matter following its application to fractional skin defects remains poorly understood, and even less is known about its in vivo impact in terms of tissue integration. The objectives of this study are twofold: (1) to evaluate the potential of calcium hydroxylapatite (CaHA) to penetrate through skin treated with a fractional laser; and (2) to assess the effectiveness of clinical laser scanning microscopy technologies in monitoring the effects of such treatment over time.

Methods: One area on a volunteer's arm was treated with a fractional erbium laser (Sciton Inc., Palo Alto, CA), while a second area received the same laser treatment followed by CaHA topical application. We used reflectance confocal microscopy (RCM) and multiphoton microscopy (MPM) to noninvasively image beneath the surface of the treated skin to study and monitor the effects of these treatments within 1 h of treatment and at four additional time points over a 6-week period.

Results: One hour posttreatment, at different depths beneath the skin surface, MPM and RCM provided similar visualizations of laser-induced channels. In skin treated by both laser and CaHA, these two imaging methods provided complementary information. RCM captured the lateral and depth distribution of CaHA microspheres and were seen as bright spheres as they became incorporated into the healing tissue. MPM, meanwhile, visualized the CaHA microparticles as dark shadow spheres within the laser-induced channels and encroaching healing tissue. Furthermore, MPM provided critical information about collagen regeneration around the microspheres, with the collagen visually marked by its distinct second harmonic generation (SHG) signal.

Conclusions: This observational pilot study demonstrates that CaHA, a collagen stimulator used as a dermal filler, can not only be inserted into the dermis after fractional laser treatment but remains in the healing skin for at least 6 weeks posttreatment. The noninvasive imaging techniques RCM and MPM successfully captured the presence of CaHA microspheres mid-dermis during the healing phase. They also demonstrated new collagen production around the microspheres, highlighting the effectiveness of these imaging approaches in monitoring such treatment over time.

1 | Introduction

In recent years, laser-assisted drug delivery (LADD) has been studied extensively for its potential to enhance the dermal uptake of topically applied agents [1–3]. Since its conceptual origin, first reported in 1987 [4], LADD has not only been studied for its applications in oncology [5, 6] and other pathological skin conditions [7, 8], but also for application in facial skin rejuvenation [9, 10]. Several studies have reported improvements in the clinical appearance of facial skin through LADD using ablative fractional lasers (AFLs) [11]. These lasers create channels in the skin surface that facilitate the rapid absorption of topically applied agents, such as hyaluronic acid (HA) [12], poly-L-lactic acid (PLLA) [11], or calcium hydroxylapatite (CaHA) [10]. As interest in LADD with AFLs grows, so does the need to better understand the delivery mechanism and the absorption of particulate materials following treatment.

An excellent article recently published by J. Cervantes et al. describes the effects on the skin of treatments using various fractional devices—including AFLs—followed by topical applications of HA, PLLA, and CaHA. The study was designed to determine the most effective topical agents and devices for filler delivery [10]. Treatments were performed on ex vivo human skin samples, and the effects were evaluated based on histological analysis. This approach raises concerns, however, about the study's conclusion that topical CaHA particles were only rarely found within the laser channels. A suggested interpretation was that this might be due to CaHA-based filler having a higher viscosity compared to other dermal fillers used as topical agents in the study, prompting it to remain localized to the skin surface. An alternative explanation could be that the microparticles were washed out during tissue processing for histological examination.

To avoid such potential misinterpretations, an ideal approach would be to perform the treatment in vivo on human skin and use one of the optical microscopy technologies currently employed in clinical skin imaging [13] to noninvasively monitor the delivery of topical agents over time. Reflectance confocal microscopy (RCM) and optical coherence tomography (OCT) have been demonstrated to effectively characterize postoperative healing of AFL-induced channels in human skin and monitor their spatio-temporal closure [9]. Furthermore, multiphoton microscopy (MPM) has proven efficient in monitoring and characterizing fractionated laser-induced optical breakdown in human skin [14].

In this study, we employ noninvasive RCM and MPM-based imaging devices in a first attempt to evaluate in vivo the potential of CaHA to be delivered through skin treated with a fractional laser. In addition, we aim to evaluate the effectiveness of these clinical laser scanning microscopy technologies in monitoring the effects of such treatment over time. The rationale for selecting these imaging approaches for a longitudinal study is based on the complementary information they provide and the unique benefits offered by the MPM device we used. The fast, large area multiphoton exoscope (FLAME), an MPM-based clinical imaging device developed in our lab, offers rapid, macroscopic imaging at a centimeter scale, allowing visualization of the entire channel grid generated by the laser treatment [15]. Furthermore, it provides specific contrast for collagen visualization, enabling visualization of new collagen formation. RCM utilizes a different contrast mechanism, enhancing the visualization of the CaHA microparticles in the skin.

2 | Materials and Methods

2.1 | Fractionated Laser Followed by Topical CaHA Application Treatment

The treatment was achieved with the Sciton erbium-doped yttrium aluminum garnet (Er:YAG) laser and its ProFractional SC scanner (Palo Alto, CA). The laser settings were 2940 nm wavelength, 430 μm beam diameter, 112.5 J/cm^2 energy density, 450 μm depth, and 60 spots/cm^2 (11%) spot density. Following the fractionated laser treatment, undiluted CaHA (Radiesse, Merz Aesthetics Inc., Raleigh, NC) was applied under occlusion. The topical CaHA was massaged into the skin for 2 min. Both areas were covered with a transparent waterproof film dressing. The area was cleaned with a gauze pad before imaging.

2.2 | Study Design

A 1×1 cm square area on the forearm of a 32-year-old volunteer was treated with the Er:YAG fractional laser. An adjacent 1×1 cm area was treated by the same laser followed by a topical application of undiluted CaHA. Imaging of these areas, as well as an untreated control area, was performed within 1 h post-treatment (Day 0), and at Weeks 1, 2, 4, and 6. All in vivo measurements were conducted according to an approved institutional review board protocol with written informed consent obtained from the subject.

2.3 | Clinical Optical Microscopy Imaging

In this longitudinal study, we utilized RCM and MPM imaging technologies to noninvasively image the treated skin areas including control. RCM, a laser-scanning imaging approach, provides sub-cellular resolution images based on differences in the refractive indices of tissue components. The clinical device used (Vivascope1500, Caliber I.D., Rochester NY, currently Vivascope, GmbH, Munich, Germany) produces grayscale 3D images beneath the skin surface over a maximum area of 8×8 mm^2.

MPM is another laser-scanning microscopy technology but employs a different contrast mechanism. In the skin, MPM contrast is derived from second harmonic generation (SHG) of collagen and two-photon excited fluorescence (TPEF) of auto-fluorescent species, including cofactors reduced nicotinamide adenine dinucleotide (NADH) and flavin adenine dinucleotide (FAD), as well as collagen, elastin, keratin, and melanin. The FLAME device used in this study was developed in our lab at the Beckman Laser Institute. It provides 3D images beneath the skin surface over a maximum area of 1×1 cm^2 with subcellular spatial resolution and label-free molecular contrast based on NADH fluorescence lifetime. Importantly, thanks to a recently implemented strip-mosaic scanning mechanism, the cm-scale skin area is mapped at a fast scan rate of about 30 s/frame.

3 | Results

On Day 0, both MPM and RCM visualized the individual defect channels generated by the fractional laser treatment as dark areas in en-face images acquired in vivo at different depths (Figure 1). The large scanning area ($1 \times 1\,cm^2$) provided by FLAME, the MPM-based device used in this study, enabled visualization of nearly the entire grid generated by the laser treatment, showing an array of approximately 8×8 fractionated channels spaced about 1 mm apart. This facilitated measurements of the defect diameters, yielding mean values of $590 \pm 170\,\mu m$ at the skin surface and $585 \pm 175\,\mu m$ at $400\,\mu m$ beneath the skin surface. The MPM imaging depth was limited to $400\,\mu m$ due to the travel range of the piezo objective scanner. Figure 1 also presents RCM images of the laser-induced channels of the treated skin. Although the RCM device offers a relatively large scanning area of $8 \times 8\,mm^2$, its acquisition time is considerably longer (several minutes) compared to the 30-s scanning time of the FLAME. The RCM images were acquired over a smaller area for comparison purposes, as the RCM and MPM contrast mechanisms are different. Thus, we used both approaches to assess the opening of the channels from superficial to deep. We found that, within 1 h posttreatment, both MPM and RCM images show that, while still open at superficial layers beneath the skin surface, many of the microchannels appeared to fill as deep as $100\,\mu m$, likely with serosanguineous fluid.

Both MPM and RCM devices were able to visualize the defects created by the laser alone. Imaging of the skin area treated with both the laser and CaHA similarly benefited from using both approaches, as they provided complementary information. RCM images were used to monitor the distribution of CaHA microparticles over time, clearly visible as bright spheres (Figure 2). Figure 2 presents RCM images of the laser and CaHA-treated skin area acquired at different depths within 1 h posttreatment (Day 0). The inset images in Figure 2d–f show a magnified image of a depth-resolved microchannel filled with a high density of microparticles. All channels showed the presence of microparticles at varying densities.

In contrast, these microparticles appeared as dark spheres in MPM images due to their lack of fluorescent signal (Figure 3). Both imaging methods showed that at Day 0, within 1 h posttreatment, the laser defect channels were open and contained CaHA microparticles at different depths, with the microparticles measuring a mean diameter of $27 \pm 4\,\mu m$.

RCM imaging was further utilized to monitor the distribution of CaHA microspheres laterally (Figure 4) and at different depths (Figure 5) as they became encapsulated by new tissue filling the defect channels over time.

Although clinically healed within a few days, the laser defects were still noticeable in the RCM images at shallow depths at Week 4
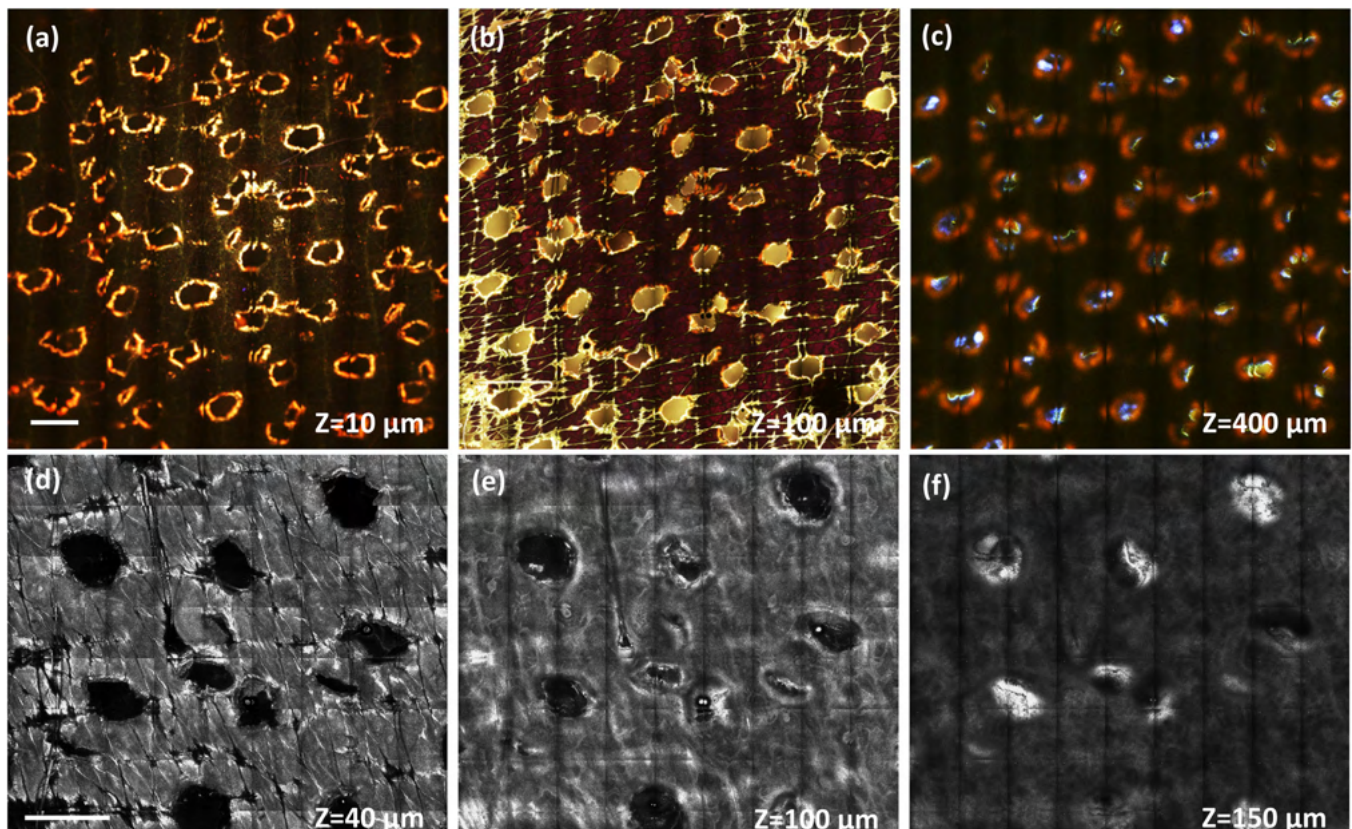

FIGURE 1 | MPM and RCM images of the laser-treated skin area at Day 0, 1 h posttreatment. Microchannels generated by the laser treatment are distinguished in both MPM (a–c) and RCM images (d–f) at different depths beneath the skin surface. While still open at superficial layers beneath the skin surface, many of the microchannels appeared to fill as deep as $100\,\mu m$ (b and e). In the MPM images, the rim of the channels is visualized through the TPEF signal from keratin, while the collagen inside the channels deeper in the dermis (c, blue) is visualized based on its SHG signal. Scale bar is 1 mm.
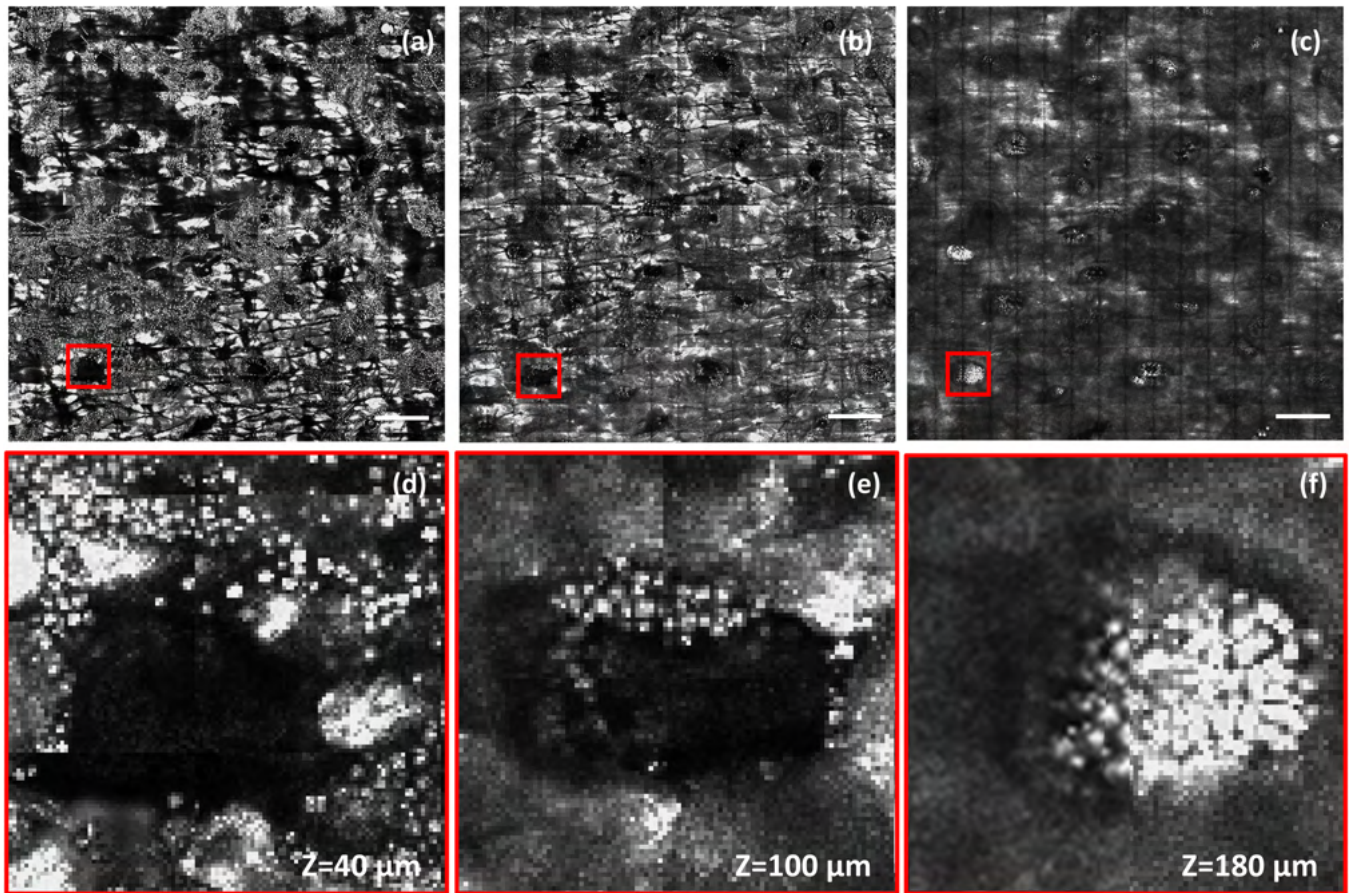
FIGURE 2 | RCM images of the laser + calcium hydroxylapatite filler-treated skin area at Day 0, 1 h posttreatment. (a–c) RCM images captured over an $8 \times 8\,mm^2$ area of the treated skin at different depths. (d–f) Inset images showing a representative microchannel filled with calcium hydroxylapatite microparticles visualized as bright spheres as deep as $180\,\mu m$. Scale bar is 1 mm.

(Figures 4d and S1). By Week 6, however, the microchannels appeared to be fully repaired at all depths, with microspheres encapsulated in the new tissue filling the channels (Figure 5).

Conversely, at Week 6, the MPM images continue to reveal well-defined microchannels undergoing repair, with collagen regeneration around the microspheres, visually marked by its distinct SHG signal (Figure 6, blue). Interestingly, the microspheres now display fluorescence, likely indicating their interaction with the skin tissue over time.

4 | Discussion

The mystique of adding biostimulatory fillers immediately after fractionated laser treatment to improve facial wrinkling and address acne scarring has been promulgated over the last decade, with some justification. However, since trends in aesthetic surgery are often little more than hope in a bottle, we should scrutinize this approach thoroughly. This scrutiny is necessary not only to validate these concepts but also to understand the underlying mechanisms and plan for optimization in the future. In medicine, there are many materials developed for tissue insertion, each potentially evoking varied degrees of foreign body reaction.

In this pilot study, we utilized RCM and MPM imaging for non-invasive, in vivo evaluation of CaHA's potential to be delivered to human skin treated with a fractional ablative laser. The main findings underscore CaHA's effectiveness in penetrating skin treated with a fractional laser that generates approximately 0.5 mm diameter microchannels. This penetration was confirmed by the presence of CaHA microparticles (sized around $25–30\,\mu m$ in diameter) within the laser microchannels, visualized across all study time points by using both RCM and MPM imaging, immediately posttreatment (Day 0) and up to Week 6 posttreatment.

A recent study by J. Cervantes et al. [10] noted, based on histological examination, the limited presence of topical CaHA particles near the surface of laser channels in human skin treated ex vivo with a fractional CO_2 laser (using a $120\,\mu m$ beam diameter) followed by CaHA microparticle application. The reasons for this limited presence of microparticles remain unclear, but potential explanations include the smaller laser channels or potential microparticle loss during histological processing.

By Week 6 posttreatment, the laser channels show signs of healing in RCM imaging. In contrast, MPM imaging at the same time point reveals that the channels remain well-defined, indicating ongoing repair as collagen regenerates around the microspheres. This regenerative process is visually distinguished by the distinctive SHG signal.

The laser channels themselves comprise a central area of vaporized tissue with a cuff of thermally denatured tissue.
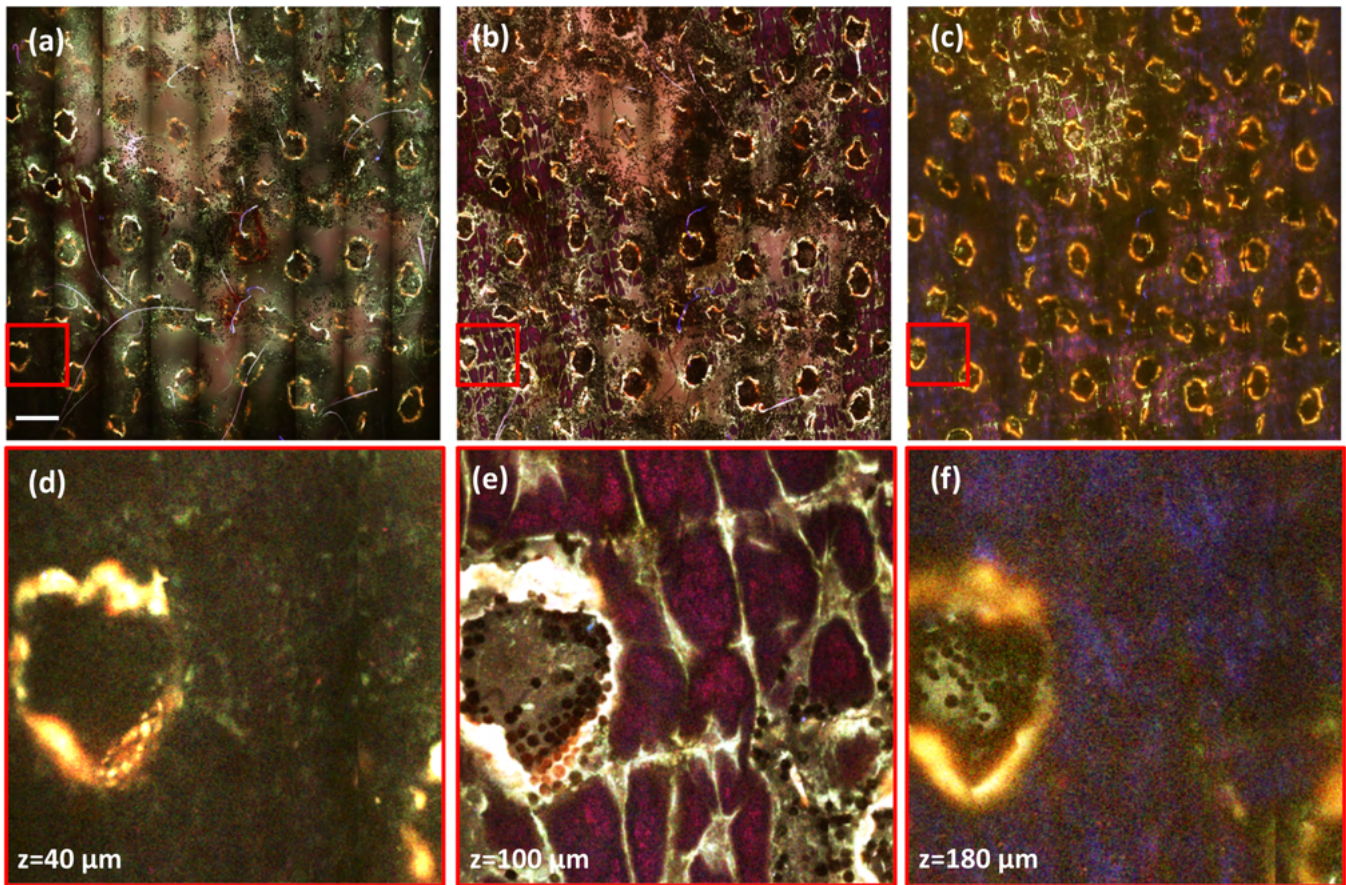
FIGURE 3 | MPM images of the laser + calcium hydroxylapatite filler-treated skin area at Day 0, 1 h posttreatment. (a–c) MPM images captured over a $10 \times 10\,\text{mm}^2$ area of the treated skin at different depths. (d–f) Inset images showing a representative microchannel filled with calcium hydroxylapatite microparticles visualized as dark spheres as deep as $180\,\mu\text{m}$. The MPM images visualize the microchannels and surrounding skin tissue based on the TPEF signal from keratin around the microchannels (d–f, yellow) and surrounding skin folds (e, yellow); TPEF signal from pigmented (melanin) basal layer (e, magenta); and SHG signal from collagen (f, blue). Scale bar is 1 mm.

It has been suggested that this cuff represents a sponge effect for drugs and allows the slow release of drugs into the local circulation. We have demonstrated that, at least with CaHA, these particles are adsorbed within the healing sponge and likely form a scaffold or stable structure upon which the skin can be rejuvenated. The acronym LADD for laser-induced drug delivery applies to the delivery of drugs, but is not accurate regarding the delivery of PLLA or CaHA, which the FDA regards as medical device implants, and which can probably be delivered by devices other than lasers. We might suggest that such a mechanism be better described by the acronym DADD, device-assisted dermal delivery.

The synergistic use of RCM and MPM imaging is evident, as CaHA microparticles are clearly visualized by RCM within the laser-induced channels, and the MPM-based FLAME device allows rapid mapping of the entire channel grid generated by the laser treatment. MPM also provides molecular contrast, allowing for visualization of new collagen formation around microparticles via SHG signal.

While promising, these results illustrate a need for further studies on cosmetically sensitive areas to assess long term the clinical impact of topical treatments. As this study was performed on only one subject's forearm, larger sample sizes would also be helpful to assess how new collagen forms in the skin from different age groups and alternative anatomical sites. Additionally, no biopsies were performed during this study due to concern for CaHA washout during histological processing. However, histologic assessment of the new collagen formation and other regenerative response changes would be of significant interest in longer longitudinal studies.

Lastly, while we have successfully demonstrated CaHA microparticles after fractionated ablative laser, it would be worthwhile exploring other agents, such as polymethyl methacrylate (PMMA) (Bellafill; Suneva, San Diego, CA), given that this is FDA-approved for acne scarring. Indeed, our understanding of foreign body reactions derives from previous studies over four decades. These indicate that an implant's characteristics dictate the reaction degree [16]. For certain devices like continuous glucose monitors and neural link electrodes, *minimal inflammatory response* is crucial, but in terms of cosmetic enhancement for thinning of the skin, *dermal plumping* is actually sought, and one can benefit from a greater immunological reaction and secondary collagen regeneration. However, the concern of granulomatous reaction should be considered and assessed in any given study.
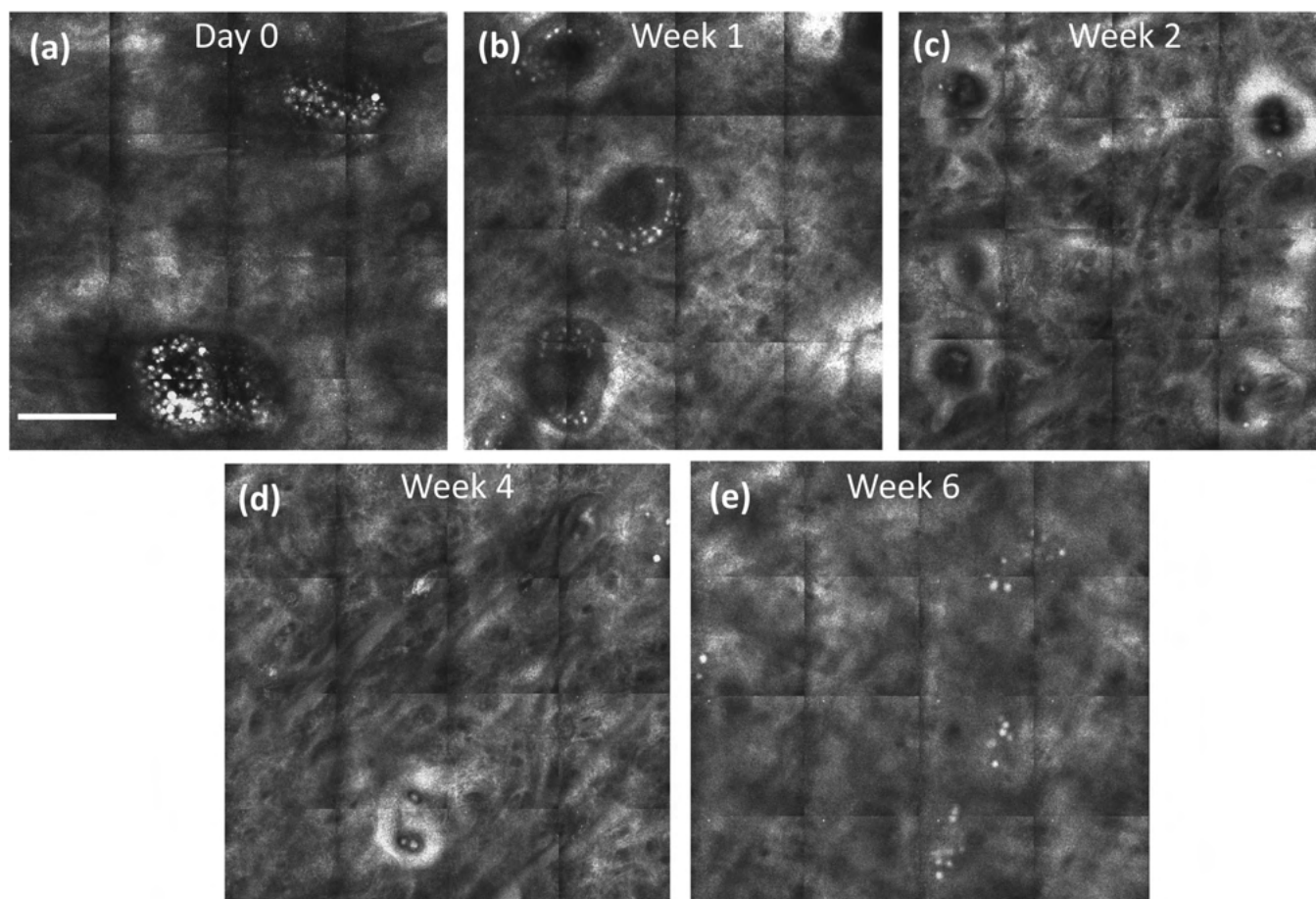
FIGURE 4 | RCM imaging of the calcium hydroxylapatite microsphere lateral distribution as they become encapsulated by new tissue over time. The images, acquired at approximately the same depth of 120–150 μm (a–e) beneath the skin surface, show calcium hydroxylapatite microspheres becoming encapsulated by new tissue, starting to fill the microchannels by Day 3 (Week 1, b) and continuing through Week 2 (c), Week 4 (d) and Week 6 (e). Scale bar is 0.5 mm.
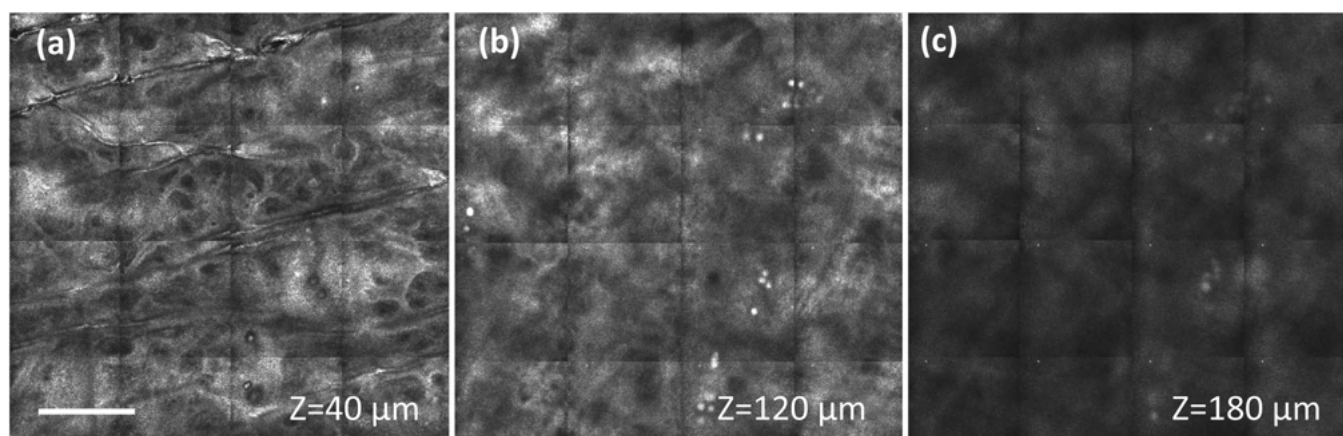

FIGURE 5 | RCM imaging of the calcium hydroxylapatite microsphere distribution at different depths as they become encapsulated by new tissue over time. The images, acquired at Week 6 posttreatment at different depths, 40 microns (a), 120 microns (b) and 180 microns (c) beneath the skin surface, show that microchannels have been repaired across all depths, with microspheres encapsulated in the new tissue filling the channels. Scale bar is 0.5 mm.

Future clinical studies will hopefully uncover the filler agents that, in association with fractionated ablative lasers, will offer optimal dermal plumping, the essence of wrinkle reduction. The latter might be referred to as Goldilocks agents..."just right."

5 | Conclusion

The era of combined fractionation and topical fillers started about 10 years ago and has been somewhat slow to reach an enthusiastic plateau. Nevertheless, this study demonstrates
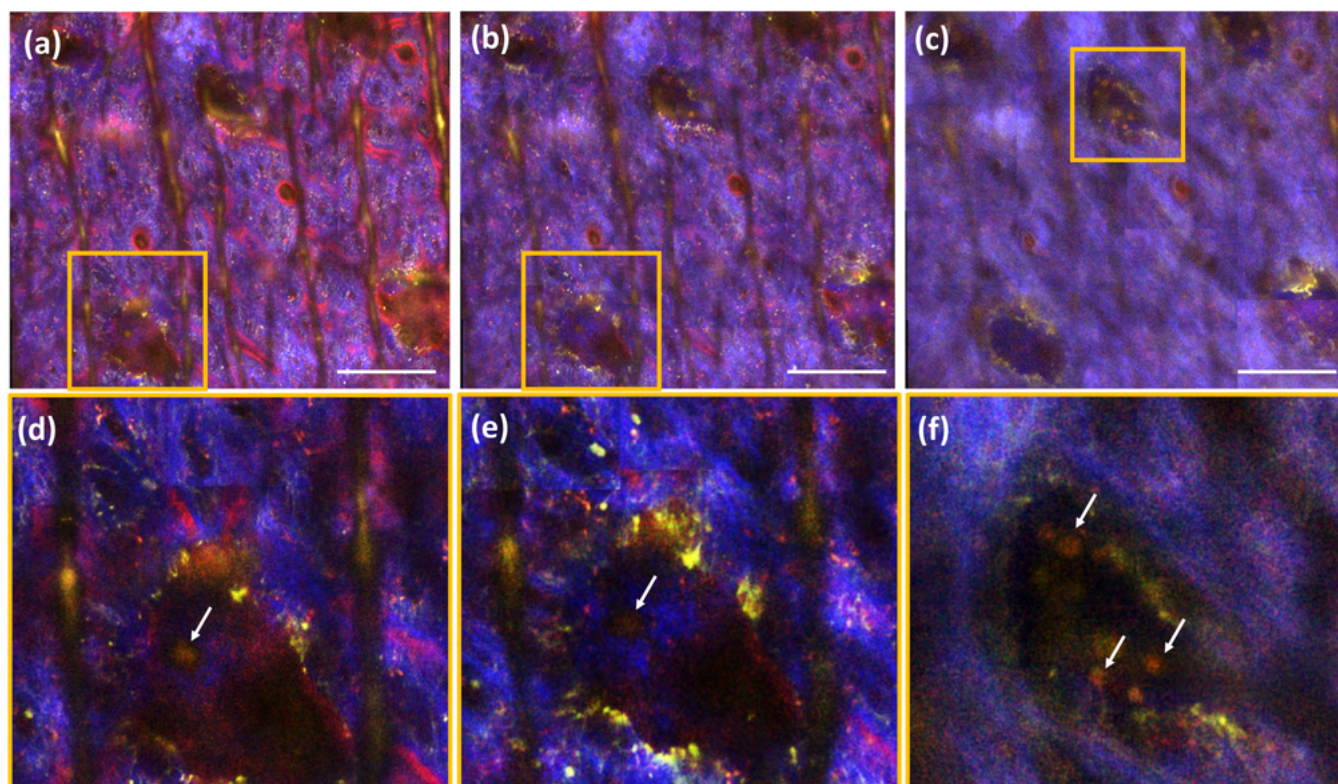
FIGURE 6 | MPM imaging of the calcium hydroxylapatite microsphere distribution at different depths as they become encapsulated by new tissue over time. The images, acquired at Week 6 posttreatment, illustrate the presence of well-delineated microchannels undergoing repair, with collagen (SHG, blue) regenerating around the microspheres (arrows) within the channels. Images were acquired at depths of 125 microns (a), 145 microns (b) and 165 microns (c) beneath the skin surface. The insets in (d), (e) and (f) show magnified views of the areas highlighted in (a), (b) and (c), respectively, providing a clearer view of the collagen surrounding the microspheres. Scale bar is 0.5 mm.

definitive advantages of the deposition of filler in the actual place where it might be most efficacious. There are ample examples of "intradermal filler" being placed in the superficial subcutaneous space, where its impact is likely less than optimal. In this study, CaHA microparticles are seen concentrated at a depth of $100–200\,\mu m$ and appear to be involved in collagen regeneration, a hallmark skin rejuvenation. This study is significant because of its in vivo nature; it has enabled us to examine and monitor the undisturbed impact of a dermal filler as the skin heals, something that hitherto was hidden from daily view.

Conflicts of Interest

M.B. is coauthor of a patent owned by the University of California, Irvine (UCI), which is related to multiphoton microscopy (MPM) imaging technology. M.B. and C.B.Z. are cofounders of Infraderm, LLC, a startup spin-off from UCI that develops MPM-based clinical imaging platforms for commercialization purposes. The Institutional Review Board and Conflict of Interest Office of the UCI have reviewed patent disclosures and did not find any concerns. The other authors declare no conflicts of interest.

References

1. E. Wenande, R. R. Anderson, and M. Haedersdal, "Fundamentals of Fractional Laser-Assisted Drug Delivery: An In-Depth Guide to Experimental Methodology and Data Interpretation," *Advanced Drug Delivery Reviews* 153 (2020): 169–184, https://doi.org/10.1016/j.addr.2019.10.003.

2. T. Searle, F. R. Ali, and F. Al-Niaimi, "Lessons Learned From the First Decade of Laser-Assisted Drug Delivery," *Dermatology and Therapy* 11 (2021): 93–104, https://doi.org/10.1007/s13555-020-00478-5.

3. W. H. S. Ng and S. D. Smith, "Laser-Assisted Drug Delivery: A Systematic Review of Safety and Adverse Events," *Pharmaceutics* 14 (2022): 2738, https://doi.org/10.3390/pharmaceutics14122738.

4. S. L. Jacques, D. J. McAuliffe, I. H. Blank, and J. A. Parrish, "Controlled Removal of Human Stratum Corneum by Pulsed Laser," *Journal of Investigative Dermatology* 88 (1987): 88–93, https://doi.org/10.1111/1523-1747.ep12465112.

5. G. Fredman, E. Wenande, K. Hendel, K. Togsverd-Bo, and M. Haedersdal, "Efficacy and Safety of Laser-Assisted Combination Chemotherapy: A Follow-Up Study of Treatment With 5-fluorouracil and Cisplatin for Basal Cell Carcinoma," *Lasers in Surgery and Medicine* 54 (2022): 113–120, https://doi.org/10.1002/lsm.23497.

6. E. Wenande, K. Hendel, M. Mogensen, et al., "Efficacy and Safety of Laser-Assisted Combination Chemotherapy: An Explorative Imaging-Guided Treatment With 5-Fluorouracil and Cisplatin for Basal Cell Carcinoma," *Lasers in Surgery and Medicine* 53 (2021): 119–128, https://doi.org/10.1002/lsm.23323.

7. A. Botsali, P. Esme, H. Erbil, and E. Caliskan, "Comparison of Fractional Erbium:Yag Laser-Assisted Tranexamic Acid Delivery Alone and in Combination With Oral Tranexamic Acid in Melasma," *Lasers in Medical Science* 37 (2022): 2823–2830, https://doi.org/10.1007/s10103-022-03547-7.

8. S. Hanthavichai, N. Archavarungson, and T. Wongsuk, "A Study to Assess the Efficacy of Fractional Carbon Dioxide Laser With Topical

Platelet-Rich Plasma in the Treatment of Androgenetic Alopecia," *Lasers in Medical Science* 37 (2022): 2279–2286, https://doi.org/10.1007/s10103-021-03496-7.

9. C. A. Banzhaf, B. S. Wind, M. Mogensen, et al., "Spatiotemporal Closure of Fractional Laser-Ablated Channels Imaged by Optical Coherence Tomography and Reflectance Confocal Microscopy," *Lasers in Surgery and Medicine* 48 (2016): 157–165, https://doi.org/10.1002/lsm.22386.

10. J. Cervantes, Y. F. Chang, J. S. Dover, A. Hernandez Alvarez, and H. J. Chung, "Laser-Assisted and Device-Assisted Filler Delivery: A Histologic Evaluation," *Dermatologic Surgery* 49 (2023): 865–870, https://doi.org/10.1097/DSS.0000000000003870.

11. A. Rkein, D. Ozog, and J. S. Waibel, "Treatment of Atrophic Scars With Fractionated CO_2 Laser Facilitating Delivery of Topically Applied Poly-L-Lactic Acid," *Dermatologic Surgery* 40 (2014): 624–631, https://doi.org/10.1111/dsu.0000000000000010.

12. M. Benzaquen, J. Fongue, V. Pauly, and A. M. Collet-Villette, "Laser-Assisted Hyaluronic Acid Delivery by Fractional Carbon Dioxide Laser in Facial Skin Remodeling: A Prospective Randomized Split-Face Study in France," *Lasers in Surgery and Medicine* 53 (2021): 1166–1172, https://doi.org/10.1002/lsm.23403.

13. G. Lentsch, E. G. Baugh, B. Lee, et al., "Research Techniques Made Simple: Emerging Imaging Technologies for Noninvasive Optical Biopsy of Human Skin," *Journal of Investigative Dermatology* 142 (2022): 1243–1252.e1, https://doi.org/10.1016/j.jid.2022.01.016.

14. M. Balu, G. Lentsch, D. Z. Korta, et al., "In Vivo Multiphoton-Microscopy of Picosecond-Laser-Induced Optical Breakdown in Human Skin," *Lasers in Surgery and Medicine* 49 (2017): 555–562, https://doi.org/10.1002/lsm.22655.

15. A. Fast, A. Lal, A. F. Durkin, et al., "Fast, Large Area Multiphoton Exoscope (FLAME) for Macroscopic Imaging With Microscopic Resolution of Human Skin," *Scientific Reports* 10 (2020): 18093, https://doi.org/10.1038/s41598-020-75172-9.

16. A. Carnicer-Lombarte, S. T. Chen, G. G. Malliaras, and D. G. Barone, "Foreign Body Reaction to Implanted Biomaterials and Its Impact in Nerve Neuroprosthetics," *Frontiers in Bioengineering and Biotechnology* 9 (2021): 622524, https://doi.org/10.3389/fbioe.2021.622524.

Supporting Information

Additional supporting information can be found online in the Supporting Information section.